A systematic comparison of all mutations in hereditary sensory neuropathy type I (HSAN I) reveals that the G387A mutation is not disease associated

— Source link ↗

Thorsten Hornemann, Anke Penno, Stephane Richard, Garth A. Nicholson ...+4 more authors

Institutions: University of Zurich, University of Antwerp

Topics: SPTLC1, Missense mutation and Mutation

Related papers:

- Hereditary sensory neuropathy type 1 is caused by the accumulation of two neurotoxic sphingolipids.

- Mutations in SPTLC1 , encoding serine palmitoyltransferase, long chain base subunit-1, cause hereditary sensory neuropathy type I

- Overexpression of the Wild-Type SPT1 Subunit Lowers Desoxysphingolipid Levels and Rescues the Phenotype of HSAN1

- SPTLC1 is mutated in hereditary sensory neuropathy, type 1

- Mutations in the yeast LCB1 and LCB2 genes, including those corresponding to the hereditary sensory neuropathy type I mutations, dominantly inactivate serine palmitoyltransferase.

A systematic comparison of all mutations in hereditary sensory neuropathy type I (HSAN I) reveals that the G387A mutation is not disease associated

Hornemann, T ; Penno, A ; Richard, S ; Nicholson, G ; van Dijk, F S ; Rotthier, A ; Timmerman, V ; von Eckardstein, A

Abstract: Hereditary sensory neuropathy type 1 (HSAN I) is an autosomal dominant inherited neurodegenerative disorder of the peripheral nervous system associated with mutations in the SPTLC1 subunit of the serine palmitoyltransferase (SPT). Four missense mutations (C133W, C133Y, V144D and G387A) in SPTLC1 were reported to cause HSAN I. SPT catalyses the condensation of Serine and Palmitoyl-CoA, which is the first and rate-limiting step in the de novo synthesis of ceramides. Earlier studies showed that C133W and C133Y mutants have a reduced activity, whereas the impact of the V144D and G387A mutations on the human enzyme was not tested yet. In this paper, we show that none of the HSAN I mutations interferes with SPT complex formation. We demonstrate that also V144D has a reduced SPT activity, however to a lower extent than C133W and C133Y. In contrast, the G387A mutation showed no influence on SPT activity. Furthermore, the growth phenotype of LY-B cells–a SPTLC1 deficient CHO cell line–could be reversed by expressing either the wild-type SPTLC1 or the G387A mutant, but not the C133W mutant. This indicates that the G387A mutation is most likely not directly associated with HSAN I. These findings were genetically confirmed by the identification of a nuclear HSAN family which showed segregation of the G387A variant as a non-synonymous SNP.

A systematic comparison of all mutations in hereditary sensory neuropathy type I (HSAN I) reveals that the G387A mutation is not disease associated

**Thorsten Hornemann · Anke Penno ·
Stephane Richard · Garth Nicholson ·
Fleur S. van Dijk · Annelies Rotthier ·
Vincent Timmerman · Arnold von Eckardstein**

Abstract Hereditary sensory neuropathy type 1 (HSAN I) is an autosomal dominant inherited neurodegenerative disorder of the peripheral nervous system associated with mutations in the SPTLC1 subunit of the serine palmitoyl-transferase (SPT). Four missense mutations (C133W, C133Y, V144D and G387A) in *SPTLC1* were reported to cause HSAN I. SPT catalyses the condensation of Serine and Palmitoyl-CoA, which is the first and rate-limiting step in the de novo synthesis of ceramides. Earlier studies showed that C133W and C133Y mutants have a reduced activity, whereas the impact of the V144D and G387A mutations on the human enzyme was not tested yet. In this paper, we show that none of the HSAN I mutations interferes with SPT complex formation. We demonstrate that also V144D has a reduced SPT activity, however to a lower extent than C133W and C133Y. In contrast, the G387A mutation showed no influence on SPT activity. Furthermore, the growth phenotype of LY-B cells—a SPTLC1 deficient CHO cell line—could be reversed by expressing either the wild-type SPTLC1 or the G387A mutant, but not the C133W mutant. This indicates that the G387A mutation is most likely not directly associated with HSAN I. These findings were genetically confirmed by the identification of a nuclear HSAN family which showed segregation of the G387A variant as a non-synonymous SNP.

Keywords HSAN I · Peripheral neuropathy · SPTLC · Serine palmitoyltransferase · Sphingolipid · Ceramide

T. Hornemann (✉) · A. Penno · S. Richard · A. von Eckardstein
Department for Clinical Chemistry, University Hospital Zurich,
Room: D-OPS33, Raemistrasse 100,
8051 Zürich, Switzerland
e-mail: thorsten.hornemann@usz.ch

G. Nicholson
Molecular Medicine Laboratory
& ANZAC Research Institute Concord,
Sydney, Australia

F. S. van Dijk
Department of Clinical Genetics, Free University Medical Center,
Amsterdam, The Netherlands

A. Rotthier · V. Timmerman
Peripheral Neuropathy Group,
VIB Department of Molecular Genetics, University of Antwerp,
Antwerp, Belgium

A. Rotthier · V. Timmerman
Neurogenetics Laboratory, Institute Born-Bunge,
University of Antwerp,
Antwerp, Belgium

Introduction

Hereditary sensory (and autonomic) neuropathy type 1 (HSN1 or HSAN I) is the most frequent HSAN subtype predominantly affecting the distal lower extremities [1]. Symptoms begin with loss of pain and temperature sensation in feet and hands, often complicated by severe infections, which can finally lead to osteomyelitis and amputations. As the disease progresses, there is degeneration of motor neurons with secondary denervation, atrophy and weakness of distal limb muscles. The mode of inheritance is autosomal dominant, with a typical onset in the second or third decade [2]. These features are characteristically associated with spontaneous, lancinating, pain attacks and deafness in some families [1]. The genetic

locus for HSAN I maps to chromosome 9q22, and positional cloning subsequently identified mutations in the *SPTLC1* gene [3, 4]. Four missense mutations (C133W, C133Y, V144D, G387A) were identified in a total of 24 HSAN I families (www.molgen.ua.ac.be/CMTMutations/) [3–5].

The *SPTLC1* gene encodes for the first of the three subunits (SPTLC1, SPTLC2 and SPTLC3) of the serine palmitoyltransferase (SPT). SPT catalyses the pyridoxal-phosphate (PLP)-dependant condensation of L-serine and palmitoyl-CoA which is the initial and rate-limiting step in the de novo synthesis of sphingolipids [6]. The two subunits SPTLC1 and SPTLC2 have a mutual similarity of 20% and are highly conserved among species. The recently identified third subunit (SPTLC3) shows 86% similarity to SPTLC2 and has a more tissue-specific distribution with very high expression levels in placenta [7]. SPTLC1 and at least one of the other two subunits are required for enzyme activity. SPTLC2 and SPTLC3 are hereby considered to be the catalytic subunits due to the presence of a PLP binding motive, which is absent in SPTLC1. The singular overexpression of SPTLC1 subunit does not change SPT activity, whereas the overexpression of the SPTLC2 or SPTLC3 subunit leads to a significant increase in cellular SPT activity [7, 8]. However, structural data indicate that the active site in SPT is located at the monomer–monomer interface and that a part of the active site is also formed by the SPTLC1 subunit [9].

Several in vitro studies show a significantly reduced SPT activity for the SPTLC1-C133W and -C133Y mutant [10–12]. For the yeast enzyme, a reduced activity was reported after introducing the V144D mutation [12]. The impact of the G387A and V144D mutation on the mammalian SPT was not investigated so far.

In this work, we intended to compare the influence of all reported HSAN I mutations on human SPT complex formation and enzyme activity to gain a better insight into the pathomechanism of this disease.

Materials and methods

Clinical data Patient CMT-820.01 is a 1-year-old child born to non-consanguineous healthy parents of Moroccan origin. The patient presented at 1 year of age with painless injuries and burns and intermitting fever episodes. The child reacts to touch, but shows insensitivity to pain stimuli. The patient developed normally. Reflexes are symmetrically low in arms and normal in legs. Electromyogram study revealed a mild, mainly sensory polyneuropathy. Informed consent was obtained from the participants and approved by the Institutional Review Board and Ethics Committees of the universities involved in this study.

Mutation analysis The coding regions and exon–intron boundaries of *SPTLC1* were polymerase chain reaction (PCR)-amplified using intronic primers as described previously [5]. Mutation screening was performed by direct sequencing of purified PCR fragments using the BigDye Terminator v3.1 cycle sequencing kit and an ABI 3730 automated capillary DNA sequencer (Applied Biosystems). The resulting sequence trace files of *SPTLC1* were aligned according to the NM_006415 sequence (NCBI) and analysed using the novoSNP program [13]. The mutation and the segregation in the family was confirmed by PCR–restriction fragment length polymorphism (PCR-RFLP) analysis using the *Eci*I restriction enzyme (New England Biolabs)

Paternity testing Paternity was tested in family CMT-820 using 15 highly informative STRs distributed throughout the genome (ATA38A05, D1S1646, D1S1653, D1S1360, D2S2256, D3S3037, D4S2382, D4S3240, D7S509, D8S1759, D9S1118, D12S1056, D12S2082, D16S2619 and GATA152H04). STRs were PCR-amplified and PCR fragments were resolved on an ABI 3730 automated DNA sequencer. Genotypes were analysed using the ABI Prism Genescan software (Applied Biosystems) and Local Geno-type Viewer, an in-house developed software program (http://www.vibgeneticservicefacility.be/).

Cloning The SPTLC1 and SPTLC2 cDNA was amplified from a human cDNA library and cloned into a pcDNA3.1D/V5-His vector as described earlier [7]. The HSAN I mutations were introduced by site-specific muta-genesis. The following primers were used for cloning:

> SPTLC1C133Wfw: 5′-ggggacccagaggattttatggcacattt gatgttc-3′
> SPTLC1C133Yfw: 5′-atggtcctcgaggattttatggcacattt gatgttc-3′
> SPTLC1V144Dfw: 5′-gtggacccagaggattttatggcacattt gatgatcatttggatttggaagaccg-3′
> SPTLC1C133W/C133Y/V144Drv: 5′-aggtacccacgcca tacttctttagagatgctaaagc-3′
> SPTLC1G387Afw: 5′-aagtggtggcggagtccctttctccagccttt cacct-3′
> SPTLC1G387Arv: 5′-ttaatccagatatcccttgtaaagctttat gaatttgtcc-3′.

All constructs were subsequently validated by sequencing (ABIPRISM™ 310 Genetic Analyser, Perkin Elmer).

Cell lines HEK293 and CHO-K1 cells were obtained from ATCC. The LY-B cell line was a gift from Dr. Kentaro Hanada (National Institute of Infectious Disease, Tokyo, Japan).

HEK293 cells were cultured in Dulbecco's modified Eagle's medium (Sigma) containing 10% fetal bovine serum (Fischer Scientific) and penicillin/streptomycin (100 U per ml/0.1 mg per ml). CHO-K1 and LY-B cells were maintained in Ham's F-12 medium (Sigma) containing 10% fetal bovine serum (Fischer Scientific) and penicillin/streptomycin (100 U per ml/0.1 mg per ml, Sigma).

Stable overexpressing cell lines HEK293 and LY-B cells were transfected with lipofectamine 2000 (Invitrogen) according to the manufacturers' instructions. The transfected cells were selected with G418 (400 μg ml^{-1}) and the expression confirmed by Western blot analysis.

Lymphoblastoid cell lines Blood samples of HSAN I patients were added to 15 ml of Ficol Paque and centrifuged for 10 min. After washing, lymphocytes were resuspended in 5 ml Epstein–Barr virus (EBV) and incubated at 37°C for 2 h. After centrifugation, the pellet was resuspended in 4 ml RPMI1640 complete medium + 1% phytohaemagglutinin. Cells were seeded in a 24-well plate and incubated at 37°C and 6% CO_2 for more than 3 days. EBV-infected cultures were observed for the appearance of clusters indicative of transformation. Cells were split and supplemented with fresh medium as needed.

Western blot For Western blot analysis, protein samples were supplemented with sodium dodecyl sulphate (SDS) loading buffer and separated by SDS–polyacrylamide gel electrophoresis (SDS-PAGE; 10% acrylamide) and blotted to a polyvinylidene fluoride (PVDF) membrane (Amersham). The membrane was blocked in Tris-buffered saline containing 0.1% Tween 20 and 5% low-fat milk powder. SPTLC1 and SPTLC2 were detected using a polyclonal rabbit serum [7]. Beta-actine and the V5-TAG were detected by commercial mouse monoclonal antibodies (Serotec). The antibodies were detected with a secondary anti-mouse/rabbit HRPO conjugate using ECL plus (Amersham) luminescence substrate. For the densitomeric analysis, the ECL reaction was directly recorded on a image analyser (Kodak Image Station 4000 MM pro) and the signal quantified using the Kodak Imaging Software.

Immunoprecipitation Cells were harvested at 70–80% confluency. The medium was removed and the cells washed twice with ice-cold phosphate-buffered saline (PBS). All steps were performed at 4°C. Cells were lysed in HT buffer [25 mM HEPES pH 8.0, 0.2% Triton X100, Protease-Inhibitors (Roche)] for 15 min followed by sonication (15 s, 50%, 0.5-s interval). Insoluble cell debris was removed by centrifugation (13,000×*g*, 5 min at 4°C). The precipitation was performed by adding 25 μl anti V5-agarose beads (Sigma). The beads were washed three times for 10 min in HT buffer (rolling at 4°C) and the bound protein eluted by adding an excess of free V5 peptide (10 mg/ml, incubated for 1 h at 4°C). The eluted proteins were separated by 12% SDS/PAGE, blotted to a PVDF membrane and the precipitated SPT subunits detected by Western blot.

Preparation of cell lysate Cells were grown on 10-cm dishes to approximately 80% confluency. Medium was removed and the cells were washed two times with PBS and harvested in 1 ml of PBS by scraping. The suspension was transferred into a 1.5-ml reaction tube. The cells were precipitated by centrifugation (2,500×*g*, 2 min at 4°C) and resolved in HT buffer [50 mM HEPES–NaOH buffer (pH 8.0), 0.2% Triton X100]. Non-solubilised components were removed by centrifugation (16,000×*g*, 5 min at 4°C). The protein concentration was adjusted to 4 mg/ml. Protein concentrations of the cell lysates were determined using the Bradford Assay (Bio-Rad). Albumin was used as a standard.

SPT Activity Assay For measuring the in vitro SPT activity, we used an improved protocol based on the published method from Dickson et al. [14]. The major alterations are the use of total cell extract instead of microsomes and the addition of 0.2% sucrose monolaurate (SML). The addition of SML results in a significantly higher specific SPT activity due to the inhibition of the interfering thioesterases background activity. Under these assay conditions, SPT activity is linear for more than 60 min, which leads to higher signals and a significantly improved signal to noise ratio. A detailed protocol about the assay is in preparation and will be published elsewhere. Typically, a reaction cocktail was composed of 400 μg total cell lysate, 50 mM HEPES (pH 8.0), 0.5 mM L-serine, 0.05 mM Palmitoyl-CoA, 20 μM Pyridoxal-5′-phosphate, 0.2% SML (Sigma), 0.1 μCi L-[U-^{14}C] serine (Amersham) in a total volume of 200 μl. The assay was performed at 37°C for 60 min. For the controls, SPT activity was specifically blocked by the addition of the SPT inhibitor myriocin (40 μM, Sigma). The reaction was stopped by adding 0.5 ml methanolic KOH/CHCl$_3$ (4:1) to the mixture. Methanolic KOH was prepared by dissolving 0.7 g KOH platelets in 100 ml MetOH. Lipids were extracted at 37°C under steady agitation for 30 min. Subsequently, 500 μl CHCl$_3$, 500 μl alkaline water [100 μl NH$_4$ (2 N) in 100 ml H$_2$O] and 100 μl NH$_4$ (2 N) were added in this order. Phases were separated by centrifugation (13,000×*g*, 5 min) and the upper phase removed. The lower phase was washed three times with alkaline water. Finally, the lower organic phase was transferred to a scintillation vial and the CHCl$_3$ evaporated under a N$_2$ steam. After the addition of scintillation cocktail, the radioactivity was quantified on a Scintillation Analyser (Packard Liquid 1900TR).

Quantitative RT-PCR The mRNA was prepared using Tri Reagent (Molecular Research Center, Cincinnati, USA) and transcribed to cDNA using oligo dT primers and Superscript III (Invitrogen) according to the manufacturer's instructions. Specific primers for the different SPT subunits were designed using the Oligo6.0 software (Molecular Biology Insights, Cascade, USA). The housekeeping gene GAPDH was used as the reference gene for quantification. Light cycler PCR was performed with a DNA Sybr-Green kit following the manufacturer's instructions (Roche Diagnostics, Basle). The following primers (0.4 μM each) were used:

SPTLC1fw: 5′-aagaagccattatatactcatat-3′; SPTLC1rv: 5′-ggcactgataagatcaata-3′
SPTLC2fw: 5′-gagtgtgtacaacagttagctg-3′; SPTLC2rv: 5′-tggctcacaaaggccac-3′.

Amplification was carried out for SPTLC1: 40 cycles, each consisting of 10 s at 95°C; 10 s at 58°C; 20 s at 72°C. SPTLC2: 40 cycles, each consisting of 10 s at 95°C; 10 s at 58°C; 20 s at 72°C. The linearity of the assays was determined by serial dilutions of the templates.

Quantification of free sphingosine bases by HPLC Cells were cultured until they reach 60–80% confluency. Lipids were extracted in the presence of the internal standard followed by an acid and base hydrolysation and quantified as OPA derivates by high-performance liquid chromatography (HPLC) and fluorescence detection. This method is based on the published protocol from Riley et al. [15].

LY-B rescue assay Stably transfected LY-B cells were seeded at a density of 7,500 cells per well in a 12-well dish. The cells were cultured overnight in Ham's F-12 medium containing 10% foetal calf serum and penicillin/streptomycin. After 24 h, the cells were washed three times with PBS and the medium exchanged to Ham's F-12 containing 1% Nutridoma-SP (Roche). After culturing the cells for 7 days, the cells were washed three times in PBS, trypsinised and counted on a coutler® Z2 cell counter (Beckman Coulter).

Results

Expression of HSAN I mutants of SPTLC1 in HEK293 cells

The SPTLC1 cDNA was amplified out of a commercial human cDNA library and cloned into a pcDNA3.1 expression vector with the fusion of a C-terminal V5-HIS tag. The four HSAN I mutations, C133W, C133Y, V144D and G387A, were introduced by site-directed mutagenesis and

the constructs transfected into HEK293 cells. Transfected cells were selected for antibiotic resistance to generate a pool of stably expressing cells. The expressed proteins were analysed by Western blot. The polyclonal SPTLC1 antibody shows a band doublet due to the mass addition of tag sequences. The lower band corresponds to the endogenous wild-type SPTLC1 and the upper band to the transfected SPTLC1 subunit (Fig. 1a). The densitometric quantification revealed no differences in the expression levels between the individual mutants. Compared to the endogenous SPTLC1 subunit, we observed a three to fivefold higher expression of the mutant. The overexpression of the SPTLC1 mutants had no influence on the expression levels of the endogenous SPTLC1 and SPTLC2 subunits (Fig. 1a).

All SPTLC1-HSAN I subunits interact with the SPTLC2 subunit

To see whether the SPTLC1-HSAN I mutations are interfering with the formation of a functional SPT complex, we
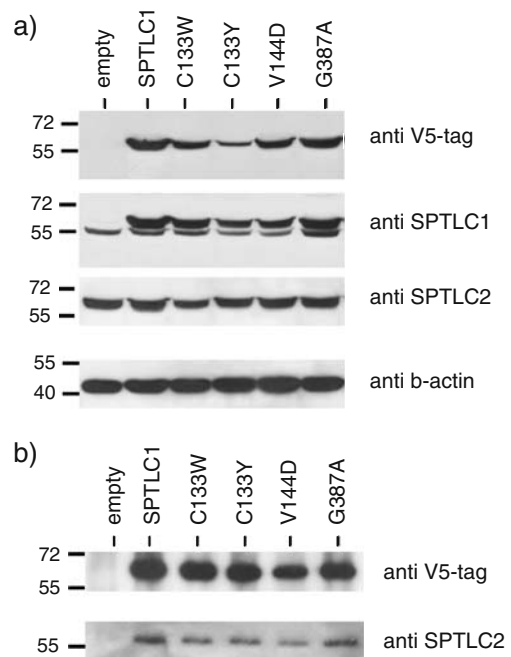

Fig. 1 **a** Western blot of HEK293 cells expressing either the empty vector, the wild-type SPTLC1 or the SPTLC1–HSAN I mutants. The transfected subunits were detected by a V5-tag antibody and a polyclonal SPTLC1 antibody. The polyclonal SPTLC1 antibody showed a band doublet due to the mass addition of the fused V5-Tag. The overexpression of SPTLC1 had no influence on the expression levels of the endogenous SPTLC1 and SPTLC2 subunit. Beta-actin immunostaining was used as a loading control. **b** Immunoprecipitation of the SPT complex in SPTLC1-HSAN I overexpressing HEK293 cells. The expressed SPTLC1 subunits were specifically precipitated with an anti V5-antibody and the precipitate probed for the co-precipitation of SPTLC2. All HSAN I mutants could be precipitated (*upper panel*) and showed a concomitant pull down of SPTLC2 (*lower panel*)

performed co-immunoprecipitation studies. The transfected SPTLC1 mutants were specifically targeted with an anti V5-tag antibody and the precipitate probed for the co-precipitation of SPTLC2. The wild-type SPTLC1 and all mutants showed a concomitant pull down of the SPTLC2 subunit (Fig. 1b). No precipitate was seen in control cells expressing the empty vector. This shows that none of the HSAN I mutations is interfering with the SPT complex formation.

SPT activity in HEK-HSAN I cells and HSAN I lymphoblasts

The influence of the HSAN I mutations on SPT activity was determined by measuring the incorporation of ^{14}C labeled

L-serine in vitro. The singular overexpression of the wild-type SPTLC1 subunit did not influence SPT activity (Fig. 2a), which is in agreement with earlier results [7]. In contrast, the overexpression of the C133W and C133Y mutant leads to a 50% reduced SPT activity (Fig. 2a). A reduced activity was also observed in V144D-expressing cells. Here, SPT activity was about 40% reduced (Fig. 2a). Surprisingly, no change in activity was observed for the G387A-expressing cells. The SPT activity in these cells was the same as in the wild-type cells (Fig. 2a).

However, the overexpression of a mutant SPTLC1 in the usual physiological context of a normal wild-type allele might not represent the situation found in HSAN I patients where only one allele is mutated. Therefore, we validated
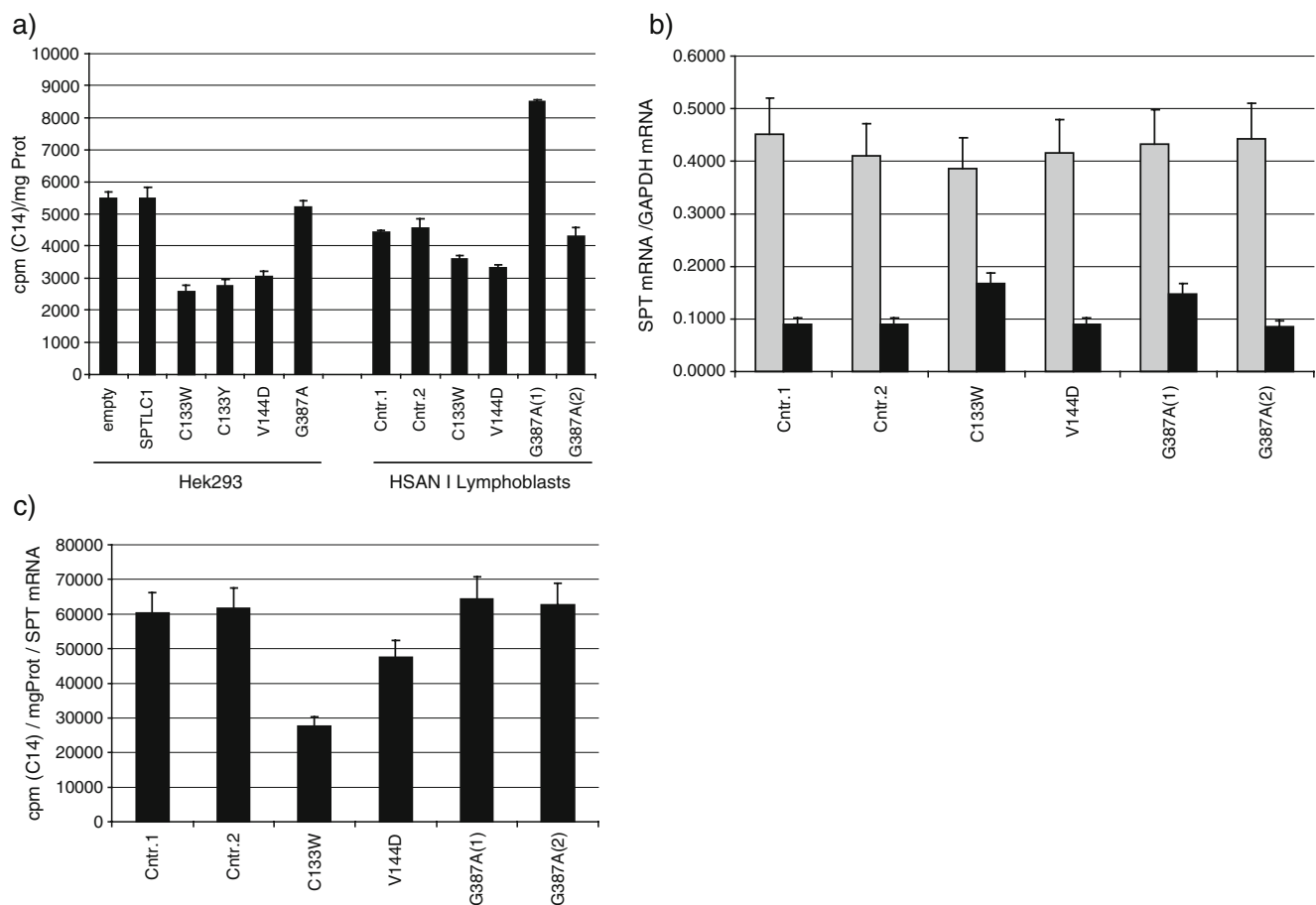

Fig. 2 **a** In vitro SPT activity in HSAN I mutant overexpressing HEK293 cells and EBV-transformed lymphoblast lines from HSAN I patients. SPT activity was significantly reduced in the HEK293 cells which expressed the C133W, C133Y and V144D mutant. Activity was unaltered in cells which expressed the wild-type SPTLC1 or the G387A variant. The activity in EBV-transformed lymphoblasts showed a different picture. Activity was less prominently reduced in the C133W lymphoblasts compared to the control lines Cntr.1 and Cntr.2. Moreover, the G387A(1) line from sister 1 showed an almost doubled activity compared to the cell line from sister 2. SPT activity in the G387A(2) line was comparable to the controls. **b** mRNA expression levels of SPTLC1 (*grey*) and SPTLC2 (*black*) in EBV-transformed HSAN I lymphoblasts. SPTLC1 mRNA expression levels were generally higher than those for SPTLC2 but not changed between the cell lines. In contrast, SPTLC2 expression levels were significantly higher in the C133W and the G387A(1) cells compared to the other lymphoblasts lines. For comparison, mRNA levels were normalised to GAPDH expression. **c** In vitro SPT activity in EBV transformed lymphoblast after normalisation to the SPTLC2 mRNA levels. The differences in SPT activity seen between G387A(1) and G387A(2) were leveled out after normalisation. The C133W line showed a more pronounced activity reduction, similar to the activity seen in the HEK293-C133W cells

these results in EBV-transformed lymphoblasts from HSAN I patients. We tested cell lines obtained from patients with a C133W and a V144D mutation and two lines from the Belgian HSAN twins (family CMT-155) in which the G387A mutation was originally reported [5]. A lymphoblast line from a C133Y carrier was not available.

Like for the mutant expressing HEK293 cells, we observed a reduced in vitro SPT activity in the cell lines from patients with C133W and V144D mutation compared to cells from unaffected controls. However, the C133W mutation seemed to have a milder impact on SPT activity in the C133W lymphoblast line compared to HEK-C133W cells (Fig. 2a). Interestingly, the two G387A lines showed contradictory results, whereas the cells from patient 1 [G387A(1)] showed a twofold increased SPT activity; the activity in the cells from patient 2 [G387A(2)] was similar to the controls (Fig. 2a). To address this discrepancy, we compared the SPTLC1 and SPTLC2 mRNA expression levels between the individual lymphoblast lines. Quantitative real-time PCR (RT-PCR) analysis revealed similar mRNA levels for SPTLC1 in all cell lines (Fig. 2b). However, the SPTLC2 mRNA levels were twofold higher in the C133W and G387A(1) cells compared to the other lines [Cntr.1, Cntr.2, V144D and G387A(2)]. This increased SPTLC2 expression in the C133W and G387A(1) lines could also be confirmed on the protein level by Western blot (data not shown). This suggests that the increased SPT activity in the C133W and the G387A(1) lymphoblast lines is caused by the augmented expression of SPTLC2 in these cells. The reason for this SPTLC2 overexpression is not clear but could possibly be caused by the previously performed EBV transformation. After the normalisation of SPT activity to the SPTLC2 mRNA expression levels, the differences between the two G387A lines are leveled out (Fig. 2c). Also, the C133W line showed a more significantly reduced SPT activity after normalisation, similar to C133W-expressing HEK293 cells.

Total sphingolipid levels are not altered in HSAN I lymphoblasts

It can be assumed that the reduced SPT activity, seen with the C133W and V144D lymphoblasts, also results in a reduced de novo synthesis and consequently in a reduced total sphingolipid content in these cells. We therefore extracted the total cellular lipids from the HSAN I lymphoblasts and subjected them to an acid and base hydrolysis. The hydrolysis under acidic conditions led to a disruption of the N-linked fatty acid and the subsequent basic hydrolysis to a release of the O-linked phosphate or carbohydrate group from the sphingosine backbone. The amount of free sphingosine was analysed by HPLC and reflected the total sphingolipid content of the cells. The

concentrations of dihydro-sphingosine (sphinganine) were negligible. Although both, the C133W and V144D lymphoblast line, showed an about 50% reduced SPT activity, we did not observe significant changes in the total sphingosine content between the HSAN I cells and the controls (Fig. 3b).

The G387A mutant can reverse the phenotype of an SPTLC1-deficient cell line

The reduced SPT activity seen in HSAN I patients is widely considered to be the pathophysiological background of HSAN I. However, this view is challenged by the observation that the G387A mutation has no impact on SPT activity. Nevertheless, the clinical symptoms of the affected sisters were reported to be typical for the HSAN I phenotype, including the presence of lancinating pain attacks which are considered as a hall mark for HSAN I. Although the G387A mutation has no impact on enzyme activity, there is still the possibility that this mutation induces other cytotoxic effects like protein aggregation or the formation of a toxic side product. To test this hypothesis, we overexpressed the G387A mutant in LY-B cells [6]. LY-B cells are mutant CHO cells which are deficient in SPT activity and de novo sphingolipid synthesis [16]. This is due to a spontaneous G246R missense mutation in the SPTLC1 subunit which renders this subunit to be unstable [17]. LY-B cells are therefore dependant on the presence of an exogenous sphingolipid source. Sufficient amounts of sphingolipids are usually provided by the added serum in the culture medium. In contrast, LY-B cells are not able to survive when the serum is replaced by a defined lipid-free serum substitute like Nutridoma SP [16]. The transfection and expression of a functional SPTLC1 subunit in LY-B cells rescues this phenotype and restores growth also in a sphingolipid-deficient medium [6]. Since the G387A mutant shows a normal in vitro activity, we presumed that this mutant should also be able to rescue the phenotype of the LY-B cells if no other cytotoxic side products are generated. We therefore expressed the G387A mutant in LY-B cells and compared the growth to SPTLC1 wild-type and C133W-expressing LY-B cells. The survival rate of the cells was analysed after cultivation for 7 days in a sphingolipid-free medium (Nutridoma SP, 1%). Untransfected LY-B cells were not able to grow under these conditions, whereas in SPTLC1-transfected cells, growth was restored and comparable to the CHO wild-type cells (Fig. 3a). The expression of the C133W mutant did not restore growth. In contrast, the expression of G387A resulted in the formation of a functional SPT enzyme and growth was fully restored. This demonstrates that the enzymatic activity of G387A is normal and sufficient to restore the de novo synthesis in the LY-B cells. It furthermore shows that the
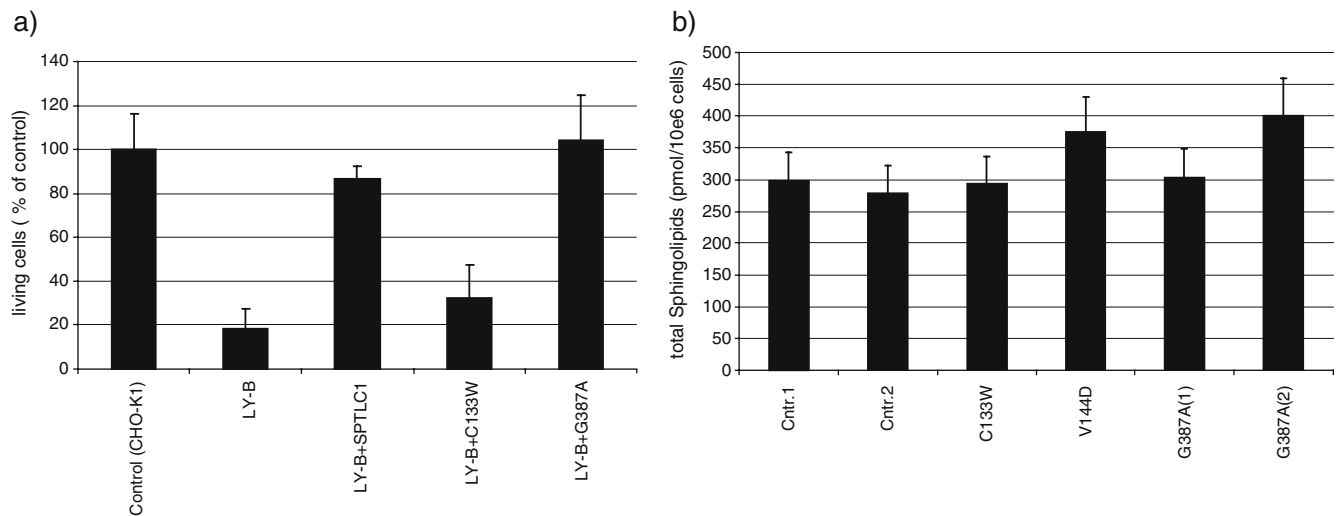
a)

b)

Fig. 3 a Restoring de novo sphingolipid synthesis in LY-B cells. Cells were stably transfected with the wild-type SPTLC1, C133W and G387A. Total cell number per dish was determined after cultivating the cells for 7 days under sphingolipid deficient conditions (Nutri-doma-SP). Whereas CHO wild-type cells could grow under these conditions, the SPTLC1-deficient LY-B cells were not able to survive without the supplementation of external sphingolipids. The transfection of the wild-type SPTLC1 subunit, but not of the inactive C133W mutant, completely reversed this restriction. Both, wild-type SPTLC1 and G387A mutant expressing LY-B cells were able to grow under these conditions. b Total sphingosine concentration in transformed HSAN I lymphoblast. Total lipids were extracted and subjected to an acid and base hydrolysis. The total sphingosine content was analysed by HPLC and normalised to cell number and C17 sphingosine, which is added as an internal standard. No significant differences in the total SO content was observed between HSAN I and control lines

expression of G387A does not induce significant toxic side effects even when the cell is fully dependent on the endogenous production of sphingolipids.

The G378A missense mutation in SPTLC1 is not necessarily associated with HSAN I

These biochemical results were finally confirmed genetically. We identified a female patient (CMT-820.01) diagnosed with a HSAN phenotype (Fig. 4a). This patient carried the same c.1160G>A variation as it was originally described in the Belgian twin sisters. This sequence variation was originally tested and found to be absent in a total of 200 unrelated control individuals. However, segregation analysis in the patients' family showed that her unaffected mother (CMT-820.03) carries the sequence variant in the homozygous state (Fig. 4b). Her father (CMT-820.2), also unaffected, carries the wild-type allele. The genetic relationship between the mother, father and their affected child was confirmed by screening a set of highly informative STR markers (data not shown).

Discussion

Initially, three SPTLC1 missense mutations (C133W, C133Y and V144D) have been reported to cause HSAN I. Later, a fourth mutation (G387A) was identified in a HSAN I family with affected twins [5]. Both patients had a typical HSAN I phenotype, including the presence of spontaneous pain attacks which is believed to be a hallmark for HSAN I. An unaffected relative did not carry the mutation.

It was previously shown that the C133W and C133Y mutations result in a decreased enzymatic activity [10–12]. In the present work, we showed that the same is true for the, not yet characterised, human V144D mutation. We therefore expected that in analogy to the other HSAN I mutants, also the G387A has an impaired activity. Surprisingly, we did not observe any changed enzymatic activity of this mutant. This was tested in G387A overexpressing HEK293 cells, but also observed in the EBV-transformed primary lymphoblast of the affected twins. The discrepancies seen for the C133W and the G387A(1) lymphoblast lines could be explained by the elevated SPTLC2 expression levels in these cells. In line with these results is the observation that the expression of G387A in the SPTLC1-deficient LY-B cells fully reverses the phenotype of these cells. This shows furthermore that the expression of the G387A mutant is also not toxic to the cell by other means.

In the light of these findings, the G387A mutation is just a benign variant of SPTLC1 and not directly disease-causing. This is further supported by the observation that this sequence variant is found in the homozygous state in the unaffected mother (CMT-820.03) of a HSAN patient (CMT-820.01). Nevertheless, it is notable that three patients with that specific sequence variation were identified by showing clinical signs of a HSAN like phenotype. This G387A mutation was found in one case out of a collective
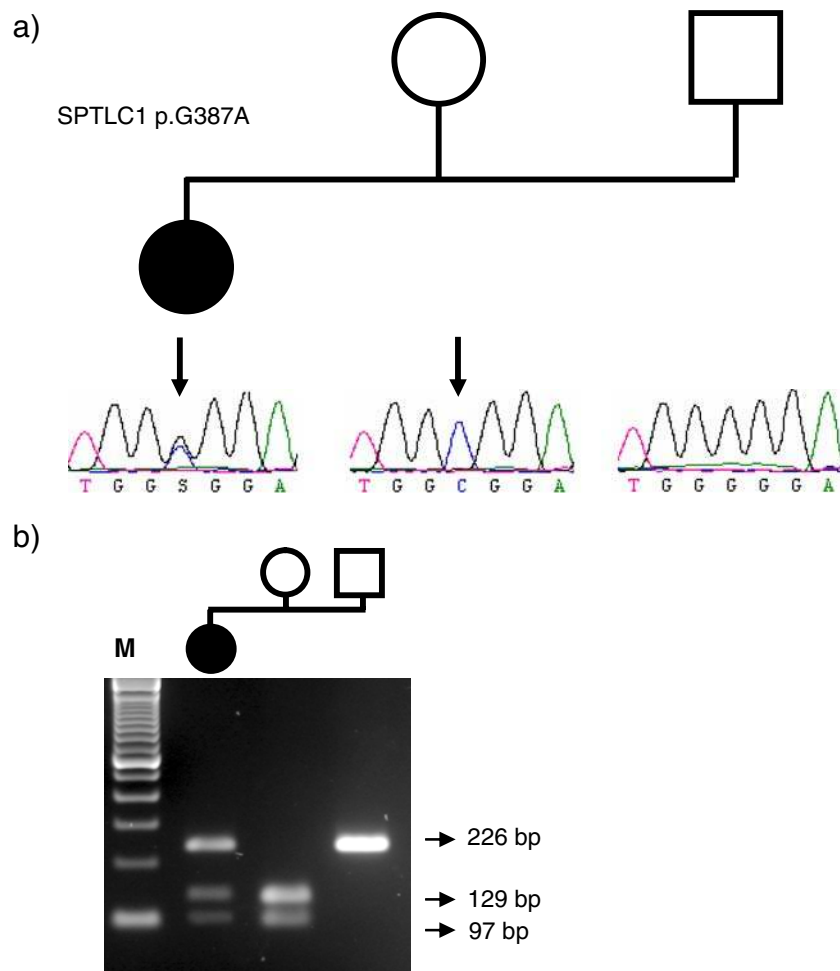
Fig. 4 The G378A missense mutation in SPTLC1 is not necessarily associated with HSAN I. We identified a female patient (CMT-820.01), diagnosed with an HSAN phenotype who carried the same c.1160G>A variation as it was originally described in the Belgian twin (**a**). This sequence variation was originally tested and found to be absent in 200 unrelated control individuals. However, segregation analysis in the patients' family showed that her unaffected mother (CMT-820.03) carries the sequence variant in the homozygous state (**a**). Her father (CMT-820.02), also unaffected, carries the wild-type allele. The screening of additional 190 unrelated control individuals revealed the presence of the G387A mutation in one of the control individuals, confirming the low frequency of this sequence variant and its benign character. **b** The c.1160G>C creates an *Eci*I restriction site of which its segregation is shown by PCR-RFLP analysis. The digested PCR product of the mothers' DNA sample shows two fragments of 129 and 97 bp, whereas the PCR product of the fathers' DNA sample remains intact (226 bp). *M* represents a 100-bp ladder

of 390 unaffected controls, indicating that it is not a frequent polymorphism. It might therefore be possible that the G387A itself is not disease-causing but has a bystander effect by increasing the risk to develop a HSAN phenotype in conjunction with another, not yet identified, mutation.

The molecular background of HSAN I is still unclear and published results are largely inconclusive and contradictory. Initially, an increase in glucosylceramide synthesis was described [4], whereas subsequently, a decreased ceramide and sphingomyelin synthesis [10, 12] and later an unchanged lipid composition was reported [11]. The latter finding is also confirmed by our own results. Interestingly, transgenic SPTLC1-C133W mice show a decreased in vitro SPT activity and develop age-dependent motor and sensory impairments [18]. Nevertheless, these mice do not show a reduction of total ceramides levels but, contrarily, an increased generation of long-chain ceramides [18]. Furthermore, heterozygous SPTLC1 and SPTLC2 knockout mice, which show a significantly reduced SPT activity [19], develop no signs of a neuropathy even at older age (Jiang X.C., personal communication). Therefore, the actual cause for HSAN1 remains unclear. Besides, there are further aspects of HSAN I which are enigmatic. Although SPT is ubiquitously expressed and essential for embryonic growth and survival [19], HSAN I is exclusively and specifically affecting the peripheral neurons. Other sphingolipid-rich organs like liver, lung or kidney appear normal in HSAN I patients. In addition, no adverse effect on the function of other neuronal tissues like the CNS was reported in HSAN I. The patients have a normal childhood

development and the late onset of the disease in the second or third decade suggests a rather mild noxious effect of the mutation.

One possible explanation would be the generation of a neurotoxic side product by the HSAN I mutants. Conversely, a direct cytotoxic effect of the other HSAN I mutants on growth or plasma membrane integrity was investigated and excluded earlier [11]. In addition, no indication for the generation of a toxic product was observed when expressing the G387A mutant in LY-B cells. Furthermore, the HSAN I mutant overexpressing HEK293 cells showed no signs of an impaired growth or survival due to the generation of a toxic metabolite. Another explanation might be the involvement of a second, yet unidentified, factor which participates in the progression of this disease. This could be, for instance, a potential interaction partner of SPT or a derailed regulatory mechanism which links the mutant SPTLC1 to the effective, but elsewhere located, pathomechanism. In this concept, the G387A mutation might also be involved, albeit the mutation itself is not directly disease-causing. In principle, all mutations found so far may alter a specific function in the peripheral nervous system that is currently not detected in lymphoblasts or other cell lines. In this context, it is interesting that two missense mutations in the RAB7 gene were reported to cause a CMT2B neuropathy which shows similar pathological features as HSAN I [20]. RAB7 belongs to the superfamily of small GTPases and is involved in endosomal trafficking. A possible interregulation of SPTLC1 and RAB7 was recently put forward [21]. However, further experiments have to be done to establish a possible pathophysiological link between those two enzymes.

References

1. Auer-Grumbach M (2008) Hereditary sensory neuropathy type I. Orphanet J Rare Dis 3:7 doi:10.1186/1750-1172-3-7
2. Dyck PJ (1993) Peripheral neuropathies. Saunders, Philadelphia, pp 1065–1093
3. Bejaoui K et al (2001) SPTLC1 is mutated in hereditary sensory neuropathy, type 1. Nat Genet 27:261–262 doi:10.1038/85817
4. Dawkins JL, Hulme DJ, Brahmbhatt SB, Auer-Grumbach M, Nicholson GA (2001) Mutations in SPTLC1, encoding serine palmitoyltransferase, long chain base subunit-1, cause hereditary sensory neuropathy type I. Nat Genet 27:309–312 doi:10.1038/85879
5. Verhoeven K et al (2004) SPTLC1 mutation in twin sisters with hereditary sensory neuropathy type I. Neurology 62:1001–1002
6. Hanada K (2003) Serine palmitoyltransferase, a key enzyme of sphingolipid metabolism. Biochim Biophys Acta 1632:16–30
7. Hornemann T, Richard S, Rutti MF, Wei Y, von Eckardstein A (2006) Cloning and initial characterization of a new subunit for mammalian serine-palmitoyltransferase. J Biol Chem 281:37275–37281 doi:10.1074/jbc.M608066200
8. Hornemann T, Wei Y, von Eckardstein A (2007) Is the mammalian serine palmitoyltransferase a high-molecular-mass complex. Biochem J 405:157–164
9. Yard BA et al (2007) The structure of serine palmitoyltransferase; gateway to sphingolipid biosynthesis. J Mol Biol 370:870–886 doi:10.1016/j.jmb.2007.04.086
10. Bejaoui K et al (2002) Hereditary sensory neuropathy type 1 mutations confer dominant negative effects on serine palmitoyltransferase, critical for sphingolipid synthesis. J Clin Invest 110:1301–1308
11. Dedov VN, Dedova IV, Merrill AH Jr, Nicholson GA (2004) Activity of partially inhibited serine palmitoyltransferase is sufficient for normal sphingolipid metabolism and viability of HSN1 patient cells. Biochim Biophys Acta 1688:168–175
12. Gable K et al (2002) Mutations in the yeast LCB1 and LCB2 genes, including those corresponding to the hereditary sensory neuropathy type I mutations, dominantly inactivate serine palmitoyltransferase. J Biol Chem 277:10194–10200 doi:10.1074/jbc.M107873200
13. Weckx S et al (2005) novoSNP, a novel computational tool for sequence variation discovery. Genome Res 15:436–442 doi:10.1101/gr.2754005
14. Dickson RC, Lester RL, Nagiec MM (2000) Serine palmitoyltransferase. Methods Enzymol 311:3–9 doi:10.1016/S0076-6879(00)11060-2
15. Riley RT, Norred WP, Wang E, Merrill AH (1999) Alteration in sphingolipid metabolism: bioassays for fumonisin- and ISP-I-like activity in tissues, cells and other matrices. Nat Toxins 7:407–414 doi:10.1002/1522-7189(199911/12)7:6<407::AID-NT84>3.0.CO;2-0
16. Hanada K et al (1998) Mammalian cell mutants resistant to a sphingomyelin-directed cytolysin. Genetic and biochemical evidence for complex formation of the LCB1 protein with the LCB2 protein for serine palmitoyltransferase. J Biol Chem 273:33787–33794 doi:10.1074/jbc.273.50.33787
17. Wei J, Yerokun T et al (2006) Sphingolipid biology. Springer, New York
18. McCampbell A et al (2005) Mutant SPTLC1 dominantly inhibits serine palmitoyltransferase activity in vivo and confers an age-dependent neuropathy. Hum Mol Genet 14:3507–3521 doi:10.1093/hmg/ddi380
19. Hojjati MR, Li Z, Jiang XC (2005) Serine palmitoyl-CoA transferase (SPT) deficiency and sphingolipid levels in mice. Biochim Biophys Acta 1737:44–51
20. Verhoeven K et al (2003) Mutations in the small GTP-ase late endosomal protein RAB7 cause Charcot–Marie–Tooth type 2B neuropathy. Am J Hum Genet 72:722–727 doi:10.1086/367847
21. Verhoeven K et al (2006) Recent advances in hereditary sensory and autonomic neuropathies. Curr Opin Neurol 19:474–480 doi:10.1097/01.wco.0000245370.82317.f6